J. Fluid Mech. (1977), *vol.* 80, *part* 3, *pp.* 443–463
Printed in Great Britain

Stokes flow in wedge-shaped trenches

By C. H. LIU AND DANIEL D. JOSEPH
Department of Aerospace Engineering and Mechanics,
University of Minnesota, Minneapolis

(Received 14 June 1976 and in revised form 1 August 1976)

In this paper we develop a separation of variables theory for solving problems of Stokes flow in wedge-shaped trenches bounded by radial lines and concentric circles centred at the vertex of the wedge. The theory leads to a set of Stokes flow eigenfunctions which in the full wedge reduce to the corner eigenfunctions studied by Dean & Montagnon (1949) and Moffatt (1964). Asymptotic formulae for the distribution of eigenvalues are derived, an adjoint system is defined and is used to develop an algorithm for the computation of the coefficients in an eigenfunction expansion of edge data prescribed on the circular boundaries. To illustrate the algorithm we find the motion and the shape of the free surface in a wedge-shaped cavity heated from its side.

1. Introduction

The aim of this paper is to contribute to a 'separation of variables' theory for Stokes flows in cavities of simple configuration. Generality in a 'separation of variables' theory is associated with the applicability of the techniques to many problems in many domains of simple shape. We claim this kind of generality for the theory given here. The techniques developed here owe much to the excellent ideas which R. C. T. Smith (1952) introduced in his study of stresses in a semi-infinite strip clamped at its side and loaded at its top edge. Smith's ideas were used by Joseph & Fosdick (1973) to study a narrow-gap approximation for secondary motions generated in the problem of the free surface on a liquid between cylinders rotating at different speeds. A more complete analysis, including numerical analysis, of the problem of Stokes flow in rectangular trenches was given by Joseph & Sturges (1975) in their study of the free surface on a liquid filling a rectangular trench heated from its side. In that paper it is shown that Smith's biorthogonal series are formally analogous to complex Fourier series and, though the biorthogonal eigenfunctions are much more complicated than circular functions, the 'Fourier coefficients' may be computed by simple algorithms. Joseph & Sturges (1975) also showed how the eigenfunction expansions should be used to compute solutions when the rectangular strip is not semi-infinite but, instead, has a solid bottom.

Smith (1952) also established conditions on the edge data sufficient to guarantee the convergence of the biorthogonal series. But Smith's conditions are too restrictive for applications. Joseph (1977) and Joseph & Sturges (1977) showed that much less restrictive conditions suffice to guarantee convergence. The biorthogonal series will converge in almost every conceivable application. The rate of convergence depends on the functions which are to be expanded. As with elementary Fourier series, convergence to 'load' functions, like step functions and ramp functions, is conditional and leads to Gibbs' phenomena.

The same types of biorthogonal expansions were used by Joseph (1974) in a study of the free surface on the round edge of a flowing liquid filling a torsion flow viscometer. This is the first case where this type of eigenfunction expansion arises for a Stokes flow problem which is not biharmonic. Similar eigenfunction expansions are required for the axisymmetric problems of Stokes flow between concentric cylinders studied by Yoo & Joseph (1977) and for the problem of axisymmetric flow in a cone studied by Liu & Joseph (1977). The study of the free surface on a viscoelastic fluid between oscillating planes (Sturges & Joseph 1977) also falls within the domain of application of the biorthogonal series. This problem may be reduced to the study of $\nabla^4\psi+\lambda^2\nabla^2\psi = 0$ (λ^2 is complex) where ψ and the normal derivative of ψ vanish on the side-walls.

The list of problems given in the last paragraph is a small sample of those which can be solved by biorthogonal eigenfunction expansions. The eigenfunctions required in these different problems depend on the given data and on the domain of flow; though the data and domains of flow differ from problem to problem, the expansions for different problems share common properties which appear to be intrinsic to Stokes flow in cavities.

In this paper we shall show how the corner eigenfunctions of Dean & Montagnon (1949) and Moffatt (1964) may be used to generate biorthogonal series solutions of Stokes flow problems in a wedge. The method is illustrated in the course of the solution which is developed for the title problem. In this example of a Stokes flow a motion is generated by buoyancy which is induced by density differences associated with heating one side-wall.

It is perhaps of interest that our work does not fully support the widely accepted view of Stokes flow in corners. We think that slow flow in a corner is determined by global considerations arising out of analysis of the entire field of flow and that there need not be eddies in corners. In our problem, the flow wedge eigenfunctions are required to turn the flow around at the free surface. No corner eddies enter the solution even though 'corner' eigenfunctions do (see figures 3, 7 and 8).

2. Mathematical formulation

The free-surface problem to be studied in the next sections is sketched in figure 1. Motion of the liquid is induced in the wedge by the driving action of density variations induced by temperature gradients. The motion is governed by the Oberbeck–Boussinesq equations in $\mathscr{V}_\epsilon$,

$$\operatorname{div}\mathbf{u} = 0, \quad \mathbf{u} = \mathbf{e}_r u_r + \mathbf{e}_\theta u_\theta,$$

$$\kappa\nabla^2 T - \mathbf{u}\,.\,\nabla T = 0, \tag{2.1a}$$

$$\mu\nabla^2\mathbf{u} + (\mathbf{e}_\theta\sin\theta - \mathbf{e}_r\cos\theta)\rho g\alpha(T-T_0) - \rho\mathbf{u}\,.\,\nabla\mathbf{u} - \nabla\Phi = 0,$$

$$\Phi = p - p_a + \rho g r\cos\theta; \tag{2.1b}$$

by the boundary conditions on the rigid walls,

$$\mathbf{u}(r, \pm\beta) = \mathbf{u}(a,\theta) = \partial T(a,\theta)/\partial r = 0, \tag{2.2a}$$

$$T(r, \pm\beta) = T_0 \pm \tfrac{1}{2}\epsilon; \tag{2.2b}$$

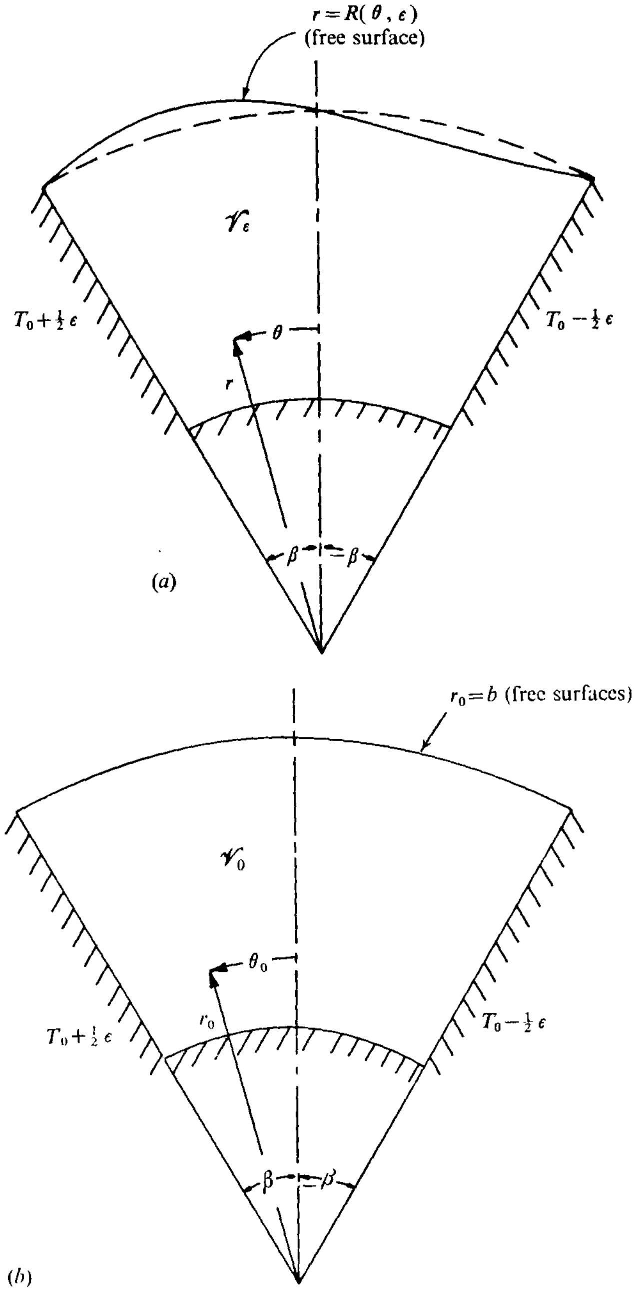

FIGURE 1. Fluid fills the sectorial region

$$\mathscr{V}_\epsilon = (r, \theta : a \leqslant r \leqslant R(\theta; \epsilon), -\beta \leqslant \theta \leqslant \beta).$$

The temperature difference between the side-walls is ϵ. The top and bottom boundaries are insulated. The configuration of $\mathscr{V}_\epsilon$ shown in (*a*) is mapped in the reference configuration $\mathscr{V}_0$ of the rest state ($R(\theta; 0) = b$, see (*b*)) by the scaling transformation:

$$r = R(\theta, \epsilon)\frac{r_0 - a}{b - a} - a\frac{r_0 - b}{b - a}, \quad \theta = \theta_0.$$

The problem is solved in $\mathscr{V}_0$.

by free-surface conditions that the free surface $r = R(\theta; \epsilon)$ is insulated, the normal component of velocity and the shear stress vanish and that the jump in the normal stress is balanced by surface tension,

$$R^2 \frac{\partial T}{\partial r} - R' \frac{\partial T}{\partial \theta} = 0, \tag{2.3a}$$

$$R u_r - R' u_\theta = 0, \tag{2.3b}$$

$$RR' \left(\frac{\partial u_r}{\partial r} - \frac{1}{r} \frac{\partial u_\theta}{\partial \theta} - \frac{u_r}{r} \right) + (R^2 - R'^2) \left(\frac{r}{2} \frac{\partial}{\partial r} \left(\frac{u_\theta}{r} \right) + \frac{1}{2r} \frac{\partial u_r}{\partial \theta} \right) = 0, \tag{2.3c}$$

$$\mu \frac{\partial u_r}{\partial r} - \Phi - \rho g R \cos\theta = \sigma J, \quad J = \frac{R^2 + 2R'^2 - RR''}{(R^2 + R'^2)^{\frac{3}{2}}}, \tag{2.3d}$$

by the requirement that $R(\theta; \epsilon)$ satisfy an adherence condition at a sharp edge,

$$R(\pm\beta; \epsilon) = 0, \tag{2.4a}$$

or a contact angle condition with horizontal contact,

$$R'(\pm\beta; \epsilon) = 0, \tag{2.4b}$$

and by the requirement that the total volume of fluid is prescribed and equal to

$$\mathscr{V}_\epsilon = \beta(b^2 - a^2) = \tfrac{1}{2} \int_{-\beta}^{\beta} R^2(\theta; \epsilon)\, d\theta. \tag{2.5}$$

The constants appearing in the equations are κ, thermal diffusivity; μ, viscosity; ρ, density; g, gravitational constant; α, thermal expansivity; T_0, reference temperature; P_a, atmospheric pressure; ϵ, temperature perturbation; σ, surface tension; $\mathscr{V}_\epsilon$, volume; β, semi-vertex angle; b, mean radius of the free surface; a, radius of wedge bottom.

Methods for relaxing condition (2.4*b*) when the prescribed angle is not flat are given by Joseph, Beavers & Fosdick (1973). When (2.4*b*) holds, it is likely that the perturbation series converges and is regular in the neighbourhood of the contact line (Sattinger 1976).

3. The perturbation series

When $\epsilon = 0$, there is no motion, $T(r, \theta) = T_0$, $\Phi = C_1$ is constant, and

$$C_1 + \rho g R \cos\theta = \sigma J, \quad \mathscr{V}_0 = \beta(b^2 - a^2), \tag{3.1}$$

where R satisfies (2.4*a*) or (2.4*b*). The solution of (3.1) gives the configuration of the rest state. Our analysis requires that $\mathscr{V}_0$ be a perfect circular sector. The solution of (3.1) is not a perfect circular sector so long as the ratio δ of the mean radius b of the free surface to the capillary radius $\delta = b/(\sigma/\rho g)^{\frac{1}{2}} \neq 0$. We shall assume that the solution can be constructed as a double power series in ϵ and δ^2. When $\epsilon = \delta = 0$, $\mathscr{V}_0$ is a perfect circular sector. The free surface is then given by

$$R(\theta; \epsilon, \delta^2) = b + R^{[0,1]}\delta^2 + R^{[1,0]}\epsilon + O(\epsilon\delta^2). \tag{3.2}$$

The function $\tilde{f}(\theta) = R^{[0,1]}$ is the static correction for small δ; that is, when the surface tension σ is large or the product $\rho g b^2$ is small. We find that

$$\tilde{f}'' + \tilde{f} + b\cos\theta = 0, \quad \int_{\beta}^{-\beta} \tilde{f}\,d\theta = 0, \quad \tilde{f}(\pm\beta) = 0, \quad \text{or} \quad \tilde{f}'(\pm\beta) = 0, \tag{3.3}$$

and $\tilde{f} = A\cos\theta - \frac{1}{2}\theta\sin\theta$ where A is to be determined from the boundary conditions.

We are interested in calculating the terms which, like $R^{[1,0]}$, are first derivatives of the solution with respect to ϵ evaluated at $(\epsilon, \delta) = (0, 0)$. This is equivalent to setting $\delta = 0$ at the outset; $\delta = 0$ has been assumed implicitly in the formulation given in §2. With $\delta = 0$ we may define the linear scaling transformation

$$r = R(\theta;\epsilon)\frac{r_0 - a}{b-a} - a\frac{r_0 - b}{b-a}. \tag{3.4}$$

Using (3.4) the deformed domain $\mathscr{V}_\epsilon$ is mapped into the reference domain. The solution of the problem in $\mathscr{V}_\epsilon$ may now be obtained as a power series whose coefficients are evaluated on the reference domain

$$\begin{pmatrix} \mathbf{u}(r,\theta;\epsilon) \\ T(r,\theta;\epsilon) \\ \Phi(r,\theta;\epsilon) \\ R(\theta;\epsilon) \end{pmatrix} = \sum_{n=0} \frac{\epsilon^n}{n!} \begin{pmatrix} \mathbf{u}^{[n]}(r_0,\theta_0) \\ T^{[n]}(r_0,\theta_0) \\ \Phi^{[n]}(r_0,\theta_0) \\ R^{[n]}(\theta_0) \end{pmatrix} \tag{3.5}$$

where
$$(\,.\,)^{[n]} = \left(\frac{\partial}{\partial\epsilon} + \frac{dr}{d\epsilon}\frac{\partial}{\partial r}\right)^n (\,.\,)$$

and $r(\epsilon)$ is given by (3.4). The term corresponding to $n = 0$ is the rest state with $\delta = 0$, $T^{[0]} = T_0$, $R^{[0]} = b$ and $\Phi^{[0]} = -\sigma/b$. It follows that

$$(\,.\,)^{[1]} = \frac{\partial(\,.\,)}{\partial\epsilon} \equiv (\,.\,)^{\langle 1\rangle},$$

and, at lowest order,

$$\begin{pmatrix} \mathbf{u}(r,\theta;\epsilon) \\ T(r,\theta;\epsilon) \\ \Phi(r,\theta;\epsilon) \\ R(\theta;\epsilon) \end{pmatrix} \sim \begin{pmatrix} 0 \\ T_0 \\ -\sigma/b \\ b \end{pmatrix} + \epsilon \begin{pmatrix} \mathbf{u}^{\langle 1\rangle}(r_0,\theta_0) \\ T^{\langle 1\rangle}(r_0,\theta_0) \\ \Phi^{\langle 1\rangle}(r_0,\theta_0) \\ R^{\langle 1\rangle}(\theta_0) \end{pmatrix}. \tag{3.6}$$

The first-order temperature correction must satisfy

$$\left.\begin{aligned} \nabla^2 T^{\langle 1\rangle} = 0 \quad \text{in} \quad \mathscr{V}_0, \\ T^{\langle 1\rangle}(r, \pm\beta) = \pm\tfrac{1}{2}, \\ \partial T^{\langle 1\rangle}(a,\theta)/\partial r = \partial T^{\langle 1\rangle}(b,\theta)/\partial r = 0, \end{aligned}\right\} \tag{3.7}$$

where we have dropped the subscripts on r_0 and θ_0. Equation (3.7) implies that

$$T^{\langle 1\rangle} = \theta/2\beta. \tag{3.8}$$

The velocity field at first order is solenoidal and satisfies

$$\mu\nabla^2\mathbf{u}^{\langle 1\rangle} + \tfrac{1}{2}\rho g(\mathbf{e}_\theta\,\theta\sin\theta - \mathbf{e}_r\,\theta\cos\theta) - \nabla\Phi^{\langle 1\rangle} = 0. \tag{3.9}$$

Introducing the stream function ψ,

$$u_r^{\langle 1\rangle} = -\frac{1}{r_0}\frac{\partial\psi}{\partial\theta}, \quad u_\theta^{\langle 1\rangle} = \frac{\partial\psi}{\partial r_0},$$

we derive, from (3.9), the governing equation

$$\nabla^4\psi = \frac{\rho\alpha g}{2\mu\beta}\frac{\cos\theta}{r_0}. \tag{3.10}$$

The boundary conditions are

$$\psi(r_0, \pm\beta) = \frac{\partial\psi}{\partial\theta}(r_0, \pm\beta) = \psi(a,\theta) = \frac{\partial\psi}{\partial r}(a,\theta) = 0, \tag{3.11}$$

and, on the free surface $r_0 = b$,

$$\psi(b,\theta) = b\frac{\partial}{\partial r_0}\left(\frac{1}{r_0}\frac{\partial\psi}{\partial r_0}(b,\theta)\right) = 0. \tag{3.12}$$

Equations (3.10), (3.11) and (3.12) determine ψ uniquely.

To reformulate the problem (3.10), (3.11) and (3.12) as an edge problem we introduce the following change of variables:

$$t = r_0/b,$$

$$\Psi(t,\theta) = \frac{2\mu\beta}{\rho\beta g b^3}\psi + \frac{t^3}{16}f(\theta,\beta), \tag{3.13a}$$

where

$$f(\theta,\beta) = \frac{1}{2\cos\beta}[(\beta+\sin\beta\cos\beta)(\cos^2\theta-\cos^2\beta)\cos\theta/\sin\beta\cos^2\beta + 2(\theta\sin\theta\cos\beta - \beta\sin\beta\cos\theta)]$$

$$= K_1\cos\theta + K_2\cos^3\theta + \theta\sin\theta, \tag{3.13b}$$

$$K_1 = -(2\beta\sin^2\beta + \tfrac{1}{2}\sin 2\beta + \beta)/\sin 2\beta$$

and

$$K_2 = (\beta + \tfrac{1}{2}\sin 2\beta)/\sin 2\beta\cos^2\beta.$$

We find that

$$\nabla^4\Psi = 0 \quad \text{in} \quad \mathscr{V}_0(t,\theta) = [t,\theta : (a/b) \leqslant t \leqslant 1, -\beta \leqslant \theta \leqslant \beta], \tag{3.14a}$$

$$\Psi(t, \pm\beta) = \frac{\partial\Psi}{\partial\theta}(t; \pm\beta) = 0, \tag{3.14b}$$

$$\Psi(1,\theta) = \frac{1}{16}f(\theta,\beta), \tag{3.14c}$$

$$\frac{\partial}{\partial t}\left(\frac{1}{t}\frac{\partial\Psi}{\partial t}(1,\theta)\right) = 3\Psi(1,\theta), \tag{3.14d}$$

$$\Psi\left(\frac{a}{b},\theta\right) = \frac{a^3}{16b^3}f(\theta,\beta), \tag{3.14e}$$

$$\frac{\partial\Psi}{\partial t}\left(\frac{a}{b},\theta\right) = \frac{3a^2}{16b^2}f(\theta,\beta). \tag{3.14f}$$

n	Complex roots λ_n ($2\beta = 10°$)	Complex roots λ_n ($2\beta = 30°$)
1	$25{\cdot}14114414 + 12{\cdot}86408537i$	$9{\cdot}06296527 + 4{\cdot}20286709i$
2	$62{\cdot}38088865 + 17{\cdot}74998684i$	$21{\cdot}46721456 + 5{\cdot}83660112i$
3	$98{\cdot}82482881 + 20{\cdot}31681729i$	$33{\cdot}61272764 + 6{\cdot}69310333i$
4	$135{\cdot}06392018 + 22{\cdot}08005326i$	$45{\cdot}69125654 + 7{\cdot}28117391i$
5	$171{\cdot}21595479 + 23{\cdot}42596613i$	$57{\cdot}74125228 + 7{\cdot}72996854i$
6	$207{\cdot}32213453 + 24{\cdot}51505806i$	$69{\cdot}77619786 + 8{\cdot}09308766i$
7	$243{\cdot}40094426 + 25{\cdot}42988724i$	$81{\cdot}80215150 + 8{\cdot}39808581i$
8	$279{\cdot}46200350 + 26{\cdot}21862740i$	$93{\cdot}82226927 + 8{\cdot}661035595i$
9	$315{\cdot}51084567 + 26{\cdot}91186944i$	$105{\cdot}83836809 + 8{\cdot}89214245i$
10	$351{\cdot}55089380 + 27{\cdot}53026222i$	$117{\cdot}83836809 + 9{\cdot}09829226i$
11	$387{\cdot}58438596 + 28{\cdot}08840449i$	$129{\cdot}86261867 + 9{\cdot}28435393i$
12	$423{\cdot}61285082 + 28{\cdot}59700027i$	$141{\cdot}87200892 + 9{\cdot}45389689i$
13	$459{\cdot}63737011 + 29{\cdot}06413212i$	$153{\cdot}88009929 + 9{\cdot}60961623i$
14	$495{\cdot}65873208 + 29{\cdot}49605305i$	$165{\cdot}88714920 + 9{\cdot}75359690i$
15	$531{\cdot}67752542 + 29{\cdot}89770025i$	$177{\cdot}89335246 + 9{\cdot}88748505i$
16	$567{\cdot}69419915 + 30{\cdot}27304019i$	$189{\cdot}89885693 + 10{\cdot}01260313i$
17	$603{\cdot}70910203 + 30{\cdot}62530754i$	$201{\cdot}90377748 + 10{\cdot}13002957i$
18	$639{\cdot}72250929 + 30{\cdot}95717482i$	$213{\cdot}90820478 + 10{\cdot}24065539i$
19	$675{\cdot}73464119 + 31{\cdot}27087556i$	$225{\cdot}91221140 + 10{\cdot}34522520i$
20	$711{\cdot}74567619 + 31{\cdot}56829546i$	$237{\cdot}91585616 + 10{\cdot}44436766i$

TABLE 1. Twenty first quadrant roots of (4.4).

4. Eigenfunctions and eigenvalues

We will construct the solution of (3.14) as a 'Fourier series' of even 'corner eigenfunctions':

$$t^{\lambda_n}\phi_1^{(n)}(\theta) \tag{4.1}$$

and

$$t^{-\lambda_n+2}\phi_1^{(n)}(\theta), \tag{4.2}$$

where

$$\phi_1^{(n)}(\theta) = \cos(\lambda_n-2)\beta\cos\lambda_n\theta - \cos\lambda_n\beta\cos(\lambda_n-2)\theta. \tag{4.3}$$

The functions (4.1) and (4.2) are on the null space of the operator

$$\nabla^4 = \left(\frac{\partial^2}{\partial t^2}+\frac{1}{t}\frac{\partial}{\partial t}+\frac{1}{t^2}\frac{\partial^2}{\partial\theta^2}\right)^2.$$

Moreover,

$$\phi_1^{(n)}(\pm\beta) = 0$$

and, if

$$\sin[2\beta(\lambda_n-1)]+(\lambda_n-1)\sin 2\beta = 0, \tag{4.4}$$

then

$$\phi_1'^{(n)}(\pm\beta) = 0.$$

There are an infinite number of first quadrant complex roots $\lambda_1, \lambda_2, \lambda_3, \ldots$, of (4.4). The roots of the equations $\sin 2\beta(\lambda-1)+(\lambda-1)\sin 2\beta = 0$ are symmetrically disposed in the four quarters of the complex $\mu = \lambda - 1$ plane, so that all roots may be obtained from the first quadrant roots.

The eigenfunctions (4.3) and eigenvalues (4.4) were studied by Dean & Montagnon (1949) and by Moffatt (1964). Dean & Montagnon (1949) noticed that when 2β is less than a critical angle 2β, say, approximately equal to 146°, equation (4.4) admits no real solutions (other than the physically irrelevant value $\mu = 0$). As 2β increases from

n	Complex roots λ_n ($2\beta = 60°$)	Complex roots λ_n ($2\beta = 90°$)
1	$5{\cdot}05932902 + 1{\cdot}95204995i$	$3{\cdot}73959336 + 1{\cdot}11902454i$
2	$11{\cdot}24572709 + 2{\cdot}77796309i$	$7{\cdot}84513517 + 1{\cdot}68163470i$
3	$17{\cdot}31416372 + 3{\cdot}20778901i$	$11{\cdot}88555236 + 1{\cdot}97019950i$
4	$23{\cdot}35138167 + 3{\cdot}50239785i$	$15{\cdot}90789082 + 2{\cdot}16733260i$
5	$29{\cdot}37518379 + 3{\cdot}72707185i$	$19{\cdot}92231201 + 2{\cdot}31746456i$
6	$35{\cdot}39187214 + 3{\cdot}90878729i$	$23{\cdot}93248783 + 2{\cdot}43880443i$
7	$41{\cdot}40429475 + 4{\cdot}06138337i$	$27{\cdot}94009829 + 2{\cdot}54065704i$
8	$47{\cdot}41394127 + 4{\cdot}19292317i$	$31{\cdot}94602973 + 2{\cdot}62843143i$
9	$53{\cdot}42167189 + 4{\cdot}30852189i$	$35{\cdot}95079721 + 2{\cdot}70555422i$
10	$59{\cdot}42802037 + 4{\cdot}41163003i$	$39{\cdot}95472195 + 2{\cdot}77433459i$
11	$65{\cdot}43333653 + 4{\cdot}50468594i$	$43{\cdot}95801537 + 2{\cdot}83640322i$
12	$71{\cdot}43785984 + 4{\cdot}58947683i$	$47{\cdot}96082267 + 2{\cdot}89295475i$
13	$77{\cdot}44176005 + 4{\cdot}66735185i$	$51{\cdot}96324707 + 2{\cdot}94489061i$
14	$83{\cdot}44516102 + 4{\cdot}73935455i$	$55{\cdot}96536410 + 2{\cdot}99290785i$
15	$89{\cdot}44815542 + 4{\cdot}80630874i$	$59{\cdot}96723038 + 3{\cdot}03755659i$
16	$95{\cdot}45081400 + 4{\cdot}86887616i$	$63{\cdot}96888923 + 3{\cdot}07927867i$
17	$101{\cdot}45319176 + 4{\cdot}92759642i$	$67{\cdot}97037437 + 3{\cdot}11843427i$
18	$107{\cdot}45533217 + 4{\cdot}98291529i$	$71{\cdot}97171252 + 3{\cdot}15532094i$
19	$113{\cdot}45727003 + 5{\cdot}03520529i$	$75{\cdot}97292509 + 3{\cdot}19018729i$
20	$119{\cdot}45903358 + 5{\cdot}08478091i$	$79{\cdot}97402945 + 3{\cdot}22324318i$

TABLE 2. Twenty first quadrant roots of (4.4).

2β to π, the number of real solutions of (4.4) increases from one to infinity. Moffatt (1964) interpreted the solutions (4.1), (4.2), (4.3) and (4.4) as a sequence of corner eddies of decreasing size and rapidly decreasing intensity. Tables 1 and 2 give the first 20 eigenvalues λ_n for wedge angles 2β of 10°, 30°, 60°, and 90°. The asymptotic formulae

$$\operatorname{Re}\lambda_n \sim 1 + (n - \tfrac{1}{4})\pi/\beta, \tag{4.5a}$$

$$\operatorname{Im}\lambda_n \sim \frac{1}{2\beta}\ln\left[k\pi(4n-1)\right], \tag{4.5b}$$

where $k = \sin 2\beta/2\beta$, approximate the real and imaginary parts of the first quadrant roots for large n. The formulae (4.5) follow from an elementary asymptotic analysis using a method introduced by Hardy (1902) and seem not to have been given before. They give rough approximations for small $n > 1$ and quite good approximations when n is large. We find, as an approximation, that

$$\operatorname{Im}\lambda_n > 0 \quad \text{when} \quad \frac{\sin 2\beta}{2\beta} > \frac{1}{\pi(4n-1)}. \tag{4.6}$$

The inequalities of (4.6) hold when $\beta < \beta_1(n)$, where

$$\frac{\sin 2\beta_1(n)}{2\beta_1(n)} = \frac{1}{\pi(4n-1)}. \tag{4.7}$$

Clearly,

$$\lim_{n\to\infty}\beta_1(n) = \pi.$$

It follows that for all values of $\beta < \pi$ there are an infinite number of complex, first quadrant eigenvalues. Moreover, we have already remarked that Dean & Montagnon

(1949) have shown that only complex roots and no real roots exist when 2β is greater than some value near 146°. The value $\beta_1(1)$, given by (4.7),

$$\frac{\sin 2\beta_1(1)}{2\beta_1(1)} = \frac{1}{3\pi},$$

is an approximation of this value.

The eigenfunctions (4.3) are even functions of θ. We study the even eigenfunctions because the edge data are even. When the edge data are odd, we could again superpose eigenfunctions (4.1) and (4.2) with $\phi_1^{(n)}(\theta)$ replaced by $\hat{\phi}_1^{(n)}(\theta)$, where

$$\hat{\phi}_1^{(n)}(\theta) = \sin(\hat{\lambda}_n - 2)\beta \sin\hat{\lambda}_n\theta - \sin\hat{\lambda}_n\beta\sin(\hat{\lambda}_n - 2)\theta.$$

The eigenvalue equation for the odd eigenfunction is

$$\sin[2\beta(\hat{\lambda}_n - 1)] - (\hat{\lambda}_n - 1)\sin 2\beta = 0. \tag{4.8}$$

It is convenient to number all of the eigenvalues λ_n which have positive real parts. Hence, we define

$$\lambda_{-n} = \bar{\lambda}_n, \tag{4.9}$$

where the overbar designates the complex conjugate. It then follows that

$$\phi_1^{(-n)}(\theta) = \overline{\phi_1^{(n)}}(\theta). \tag{4.10}$$

5. Solution of the edge problem

The solution of (3.14) can be written as

$$\Psi = \sum_{-\infty}^{\infty} [C_n t^{\lambda_n} + D_n t^{-\lambda_n+2}]\,\phi_1^{(n)}(\theta)/\lambda_n(\lambda_n - 2), \tag{5.1}$$

where $C_0 = D_0 = 0$ and, since the given edge data are real and $\lambda_{-n} = \bar{\lambda}_n$ and

$$\phi_1^{(-n)}(\theta) = \bar{\phi}_1^{(n)}(\theta), \quad C_{-n} = \bar{C}_n \quad \text{and} \quad D_{-n} = \bar{D}_n.$$

Equation (5.1) is biharmonic and satisfies the side-wall boundary conditions. We must show that the coefficients C_n and D_n can be selected such that (5.1) satisfies the given conditions at the bottom $t = a/b$ and at the top $t = 1$. It is convenient to consider the special case $a = 0$ first.

5.1. *The full sector* ($a = 0$)

When $a = 0$ the velocities corresponding to (5.1) are unbounded as $t \to 0$. To obtain a bounded velocity we set $D_n = 0$ for all n. We next introduce the boundary data vector

$$\mathbf{f} = \begin{pmatrix} f(\theta) \\ g(\theta) \end{pmatrix} = \begin{pmatrix} \partial\left(\frac{1}{t}\,\partial\Psi/\partial t\right)\Big/\partial t \\ \partial^2\Psi/\partial\theta^2 \end{pmatrix}_{t=1} \tag{5.2}$$

$$= \frac{1}{16}\begin{pmatrix} 3f(\theta,\beta) \\ -K_1\cos\theta - 3K_2\cos\theta(3\sin^2\theta - 1) + 2\cos\theta - \theta\sin\theta \end{pmatrix}.$$

The given edge condition (5.2) is compatible with the side-wall boundary conditions (for a full discussion, see Joseph (1977))

$$\int_{-\beta}^{\beta} g(\theta)\,d\theta = \int_{-\beta}^{\beta} \theta g(\theta)\,d\theta = 0. \tag{5.3}$$

The boundary data (5.2) are now expanded in a series of eigenfunctions

$$\begin{pmatrix} f \\ g \end{pmatrix} = \sum_{-\infty}^{\infty} C_n \begin{pmatrix} \phi_1^{(n)} \\ \phi_2^{(n)} \end{pmatrix} \tag{5.4}$$

where
$$\phi_2^{(n)} = \frac{1}{\lambda_n(\lambda_n-2)}\,\phi_1''^{(n)}. \tag{5.5}$$

To determine the constants C_n we introduce the vectors

$$\boldsymbol{\varphi}^{(n)} = \begin{pmatrix} \phi_1^{(n)} \\ \phi_2^{(n)} \end{pmatrix}, \quad \boldsymbol{\psi}^{(n)} = [\psi_1^{(n)}, \psi_2^{(n)}]. \tag{5.6}$$

The vector $\boldsymbol{\varphi}^{(n)}$ satisfies the differential equation

$$\boldsymbol{\varphi}''^{(n)} + \mathbf{A}_n . \boldsymbol{\varphi}^{(n)} = 0, \tag{5.7}$$

where
$$\mathbf{A}_n = \begin{pmatrix} 0 & -\lambda_n(\lambda_n-2) \\ \lambda_n(\lambda_n-2) & (\lambda_n-2)^2+\lambda_n^2 \end{pmatrix},$$

and the boundary conditions $\phi_1^{(n)}(\pm\beta) = \phi_1'^{(n)}(\pm\beta) = 0$. The adjoint vector $\boldsymbol{\psi}^{(n)}$ satisfies the differential equation

$$\boldsymbol{\psi}''^{(n)} + \boldsymbol{\psi}^{(n)} . \mathbf{A}_n = 0 \tag{5.8}$$

and the boundary conditions $\psi_2^{(n)}(\pm\beta) = \psi_2'^{(n)}(\pm\beta) = 0$. We find that

$$\left.\begin{aligned} \psi_2^{(n)} &= \phi_1^{(n)}, \\ \phi_2^{(n)} &= \frac{(\lambda_n-2)}{\lambda_n}\cos\lambda_n\beta\cos(\lambda_n-2)\theta - \frac{\lambda_n}{(\lambda_n-2)}\cos(\lambda_n-2)\beta\cos\lambda_n\theta, \\ \text{and}\quad \psi_1^{(n)} &= \frac{(\lambda_n-2)}{\lambda_n}\cos(\lambda_n-2)\beta\cos\lambda_n\theta - \frac{\lambda_n}{(\lambda_n-2)}\cos\lambda_n\beta\cos(\lambda_n-2)\theta. \end{aligned}\right\} \tag{5.9}$$

From (5.7) and (5.8) and the boundary conditions we find the following property of biorthogonality:

$$\int_{-\beta}^{\beta} \boldsymbol{\psi}^{(m)} . \mathbf{A} . \boldsymbol{\varphi}^{(n)} d\theta = 0 \quad \text{if} \quad (\lambda_n-1)^2 \neq (\lambda_m-1)^2, \tag{5.10}$$

where
$$\mathbf{A} = \begin{pmatrix} 0 & -1 \\ 1 & 2 \end{pmatrix}.$$

Using (4.3) and (5.9) we compute

$$\begin{aligned} \int_{-\beta}^{\beta} \boldsymbol{\psi}^{(n)} . \mathbf{A} . \boldsymbol{\varphi}^{(n)} d\theta = F_n = 4\Bigg\{ &\frac{\beta\cos^2\lambda_n\beta}{\lambda_n} - \frac{\beta\cos^2(\lambda_n-2)\beta}{(\lambda_n-2)} \\ &- \frac{2(\lambda_n-1)^2\sin 2\beta\cos\lambda_n\beta\cos(\lambda_n-2)\beta}{\lambda_n^2(\lambda_n-2)^2} \\ &- \frac{(\lambda_n^2-2\lambda_n+2)\cos\lambda_n\beta\cos(\lambda_n-2)\beta\sin 2(\lambda_n-1)\beta}{\lambda_n^2(\lambda_n-1)(\lambda_n-2)^2}\Bigg\}. \end{aligned} \tag{5.11}$$

θ	$f(\theta)$	$N = 1$	$N = 3$	$N = 5$	$N = 9$	$N = 10$
0°	0·06267	0·02035	0·05420	0·05949	0·06159	0·06359
3°	0·05769	0·04210	0·05307	0·06074	0·05650	0·05862
6°	0·04404	0·08416	0·04327	0·04143	0·04255	0·04495
9°	0·02543	0·09584	0·01406	0·02705	0·02369	0·02627
12°	0·00799	0·04903	0·02715	0·00834	0·00650	0·00861
12°	0	0	0	0	0	0
θ	$g(\theta)$	$N = 1$	$N = 3$	$N = 5$	$N = 9$	$N = 10$
0°	−1·235	−1·249	−1·229	−1·232	−1·234	−1·235
3°	−1·081	−1·098	−1·086	−1·083	−1·080	−1·082
6°	−0·626	−0·634	−0·622	−0·624	−0·624	−0·626
9°	0·1187	0·1458	0·1222	0·1189	0·1205	0·1182
12°	1·1296	1·1740	1·1208	1·1260	1·1330	1·1298
15°	2·3770	2·2343	2·3636	2·3732	2·3760	2·3761

TABLE 3. Convergence of the partial sums of the series (5.14) for wedge angle of 30°:
$$\begin{pmatrix} f \\ g \end{pmatrix} = 10^2 \times \sum_{-N}^{N} C_n \begin{pmatrix} \phi_1^{(n)} \\ \phi_2^{(n)} \end{pmatrix}.$$

With these preliminaries aside we may now use the biorthogonality conditions (5.10) and (5.11) to compute the C_n. Recalling that $\mathbf{f} = \Sigma\, C_n \boldsymbol{\varphi}^{(n)}$, we find that

$$I_n \equiv \int_{-\beta}^{\beta} \boldsymbol{\psi}^{(n)} . \mathbf{A} . \mathbf{f}\, d\theta = C_n F_n. \tag{5.12}$$

The integral I_n is computed using (5.2) and (5.9). We find that

$$I_n = \tfrac{1}{16}[P_n \cos(\lambda_n - 2)\beta + Q_n \cos\lambda_n \beta], \tag{5.13a}$$

where

$$\begin{aligned} P_n = {} & \left(3K_1 + \frac{\lambda_n+2}{\lambda_n}(-K_1+6K_2+2)\right)\left(\frac{\sin(\lambda_n-1)\beta}{\lambda_n-1} + \frac{\sin(\lambda_n+1)\beta}{\lambda_n+1}\right) \\ & + \tfrac{3}{4}K_2\left(1 - 3\frac{(\lambda_n+2)}{\lambda_n}\right)\left(\frac{\sin(\lambda_n-3)\beta}{\lambda_n-3} + \frac{\sin(\lambda_n+3)\beta}{\lambda_n+3}\right. \\ & \left. + \frac{3\sin(\lambda_n-1)\beta}{\lambda_n-1} + \frac{3\sin(\lambda_n+1)\beta}{\lambda_n+1}\right) \\ & + \left(3 - \frac{\lambda_n+2}{\lambda_n}\right)\left(\frac{\sin(\lambda_n+1)\beta}{(\lambda_n+1)^2} - \frac{\beta\cos(\lambda_n+1)\beta}{\lambda_n+1}\right. \\ & \left. - \frac{\sin(\lambda_n-1)\beta}{(\lambda_n-1)^2} + \frac{\beta\cos(\lambda_n-1)\beta}{\lambda_n-1}\right), \end{aligned} \tag{5.13b}$$

$$\begin{aligned} Q_n = {} & \left(-3K_1 + \frac{4-\lambda_n}{\lambda_n-2}(-K_1+6K_2+2)\right)\left(\frac{\sin(\lambda_n-3)\beta}{\lambda_n-3} + \frac{\sin(\lambda_n-1)\beta}{\lambda_n-1}\right) \\ & - \tfrac{3}{4}K_2\left(1 + 3\frac{4-\lambda_n}{\lambda_n-2}\right)\left(\frac{\sin(\lambda_n-5)\beta}{\lambda_n-5} + \frac{\sin(\lambda_n+1)\beta}{\lambda_n+1}\right. \\ & \left. + \frac{3\sin(\lambda_n-3)\beta}{\lambda_n-3} + \frac{3\sin(\lambda_n-1)\beta}{\lambda_n-1}\right) \\ & - \left(3 + \frac{4-\lambda_n}{\lambda_n-2}\right)\left(\frac{\sin(\lambda_n-1)\beta}{(\lambda_n-1)^2} - \frac{\beta\cos(\lambda_n-1)\beta}{(\lambda_n-1)}\right. \\ & \left. - \frac{\sin(\lambda_n-3)\beta}{(\lambda_n-3)^2} + \frac{\beta\cos(\lambda_n-3)\beta}{(\lambda_n-3)}\right). \end{aligned} \tag{5.13c}$$

θ	$f(\theta)$	$N=1$	$N=3$	$N=5$	$N=9$	$N=10$
0°	0·12356	0·10503	0·12021	0·12233	0·12314	0·12393
6°	0·11340	0·10620	0·11615	0·11459	0·11293	0·11377
12°	0·08575	0·10202	0·08555	0·08473	0·08517	0·08611
18°	0·04875	0·07757	0·04433	0·04940	0·04809	0·04909
24°	0·01498	0·03160	0·02213	0·01505	0·01445	0·01526
30°	0	0	0	0	0	0
θ	$g(\theta)$	$N=1$	$N=3$	$N=5$	$N=9$	$N=10$
0°	−0·6322	−0·6350	−0·6299	−0·6312	−0·6318	−0·6325
6°	−0·5455	−0·5506	−0·5477	−0·5465	−0·5451	−0·5459
12°	−0·2953	−0·3002	−0·2941	−0·2941	−0·2947	−0·2956
18°	0·09046	0·09824	0·09202	0·09047	0·09116	0·09023
24°	0·56803	0·58484	0·56453	0·56675	0·56880	0·56806
30°	1·0835	1·0319	1·0780	1·0812	1·0821	1·0822

TABLE 4. Convergence of the partial sums of the series (5.14) for wedge angle of 60°:

$$\begin{pmatrix} f \\ g \end{pmatrix} = 10 \times \sum_{-N}^{N} C_n \begin{pmatrix} \phi_1^{(n)} \\ \phi_2^{(n)} \end{pmatrix}.$$

In tables 3 and 4 we have the convergence of the partial sums

$$\mathbf{f} \sim \sum_{-N}^{N} C_n \boldsymbol{\varphi}^{(n)}(\theta) \tag{5.14}$$

as a function of the truncation number when $2\beta = 30°$ and $2\beta = 60°$. The rapid convergence evident in these tables is characteristic of all the results ($10° < 2\beta < 90°$) computed by us. A good representation can be obtained in two terms.

Mathematical convergence may be established by application of the theorem of Joseph (1977) which holds for edge data satisfying (5.3) and the conditions

$$f(\pm\beta,\beta) = f'(\pm\beta,\beta) = 0. \tag{5.15}$$

Equation (5.15) may be verified most easily by using the first of the forms of $f(\theta,\beta)$ given by (3.13b). The representations (5.13) are not optimal for the demonstration of rapid mathematical convergence. To demonstrate rapid mathematical convergence from (2.13b) we must account for cancellations at large values of n. It is much easier to demonstrate mathematical convergence using the first of the forms of $f(\theta,\beta)$ given by (3.13b). The integrals I_n are integrated twice by parts using (5.15). This integration by parts puts a factor whose largest terms are $O(\lambda_n^2)$ in the denominator of the C_n, ensuring rapid convergence. To be precise, the asymptotic representations (4.5a,b) imply that when n is large

$$\cos\lambda_n\beta \quad \text{and} \quad \sin\lambda_n\beta \quad \text{are} \quad O(n^{\frac{1}{2}})$$

and

$$I_n = O(1/n^3).$$

On taking account of cancellations

$$F_n = O(1), \quad C_n = O(1/n^3)$$

and

$$C_n\phi_1^{(n)}(\theta) = O(1/n^2).$$

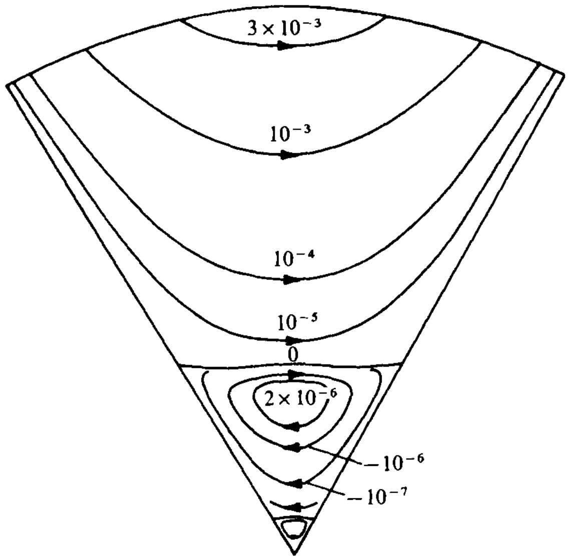

FIGURE 2. Level lines of the edge eddies (5.6) in the reference domain. Wedge angle 2β is 60°.

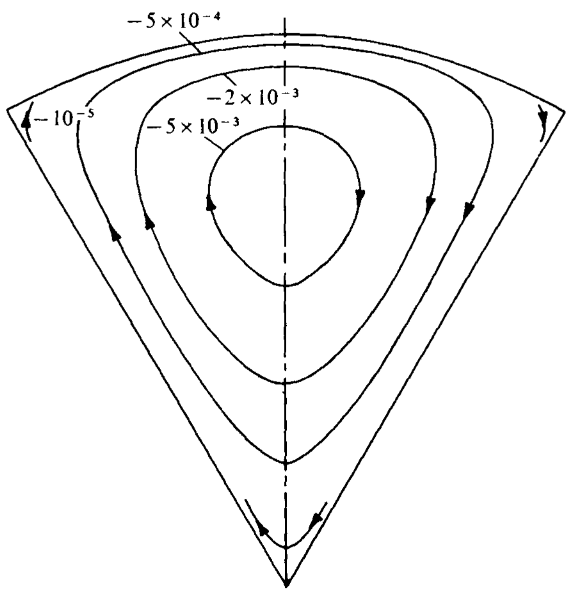

FIGURE 3. Streamlines (5.19) of the flow in the reference domain. Wedge angle 2β is 60°.

The convergence of the series

$$\Psi = \sum_{-\infty}^{\infty} C_n t^{\lambda_n} \phi_1^{(n)}(\theta)/\lambda_n(\lambda_n - 2) \tag{5.16}$$

is even more rapid; it is dominated by terms of order C/n^4, at least.

The expression (5.16) gives the edge eddies. These eddies are required to turn the stream around at the edge. The real stream function $\psi(t, \theta)$, given by (3.13*a*), is

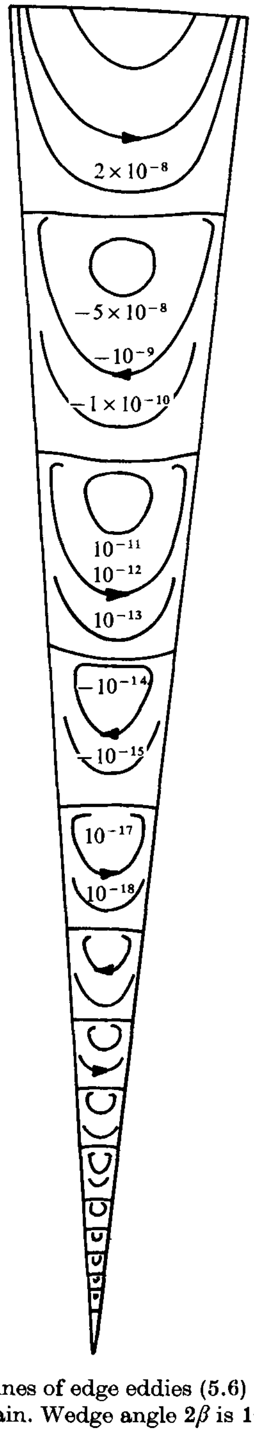

FIGURE 4. Level lines of edge eddies (5.6) in the reference domain. Wedge angle 2β is $10°$.

θ	$\frac{10^6 \times f(\theta,\beta)}{16}$	$N = 1$	$N = 3$	$N = 5$	$N = 9$	$N = 10$
			On the top: $t = 1$			
0°	2·43372	2·44776	2·43352	2·43363	2·43368	2·43369
1°	2·24267	2·25377	2·24292	2·24268	2·24263	2·24264
2°	1·71647	1·71889	1·71609	1·71642	1·71642	1·71644
3°	0·99585	0·98791	0·99574	0·99579	0·99581	0·99583
4°	0·31485	0·30605	0·31550	0·31492	0·31481	0·31482
5°	0	0	0	0	0	0
			On the bottom: $t = 0{\cdot}5$			
0°	2·43372	2·32407	2·44525	2·43388	2·43340	2·43369
1°	2·24267	2·18042	2·24255	2·24250	2·24235	2·24263
2°	1·71647	1·75339	1·71876	1·71639	1·71617	1·71644
3°	0·99585	1·09052	0·99426	0·99620	0·99560	0·99583
4°	0·31485	0·37174	0·31285	0·31407	0·31468	0·31482
5°	0	0	0	0	0	0

TABLE 5. Convergence of the top edge series (6.1) and the bottom edge series (6.2) when $2\beta = 10°$ and $a/b = 0{\cdot}5$.

$$\frac{\Psi}{t^3} \times 10^6 = \frac{10^6 \times f(\theta,\beta)}{16} = 10^6 \times \sum_{-N}^{N} (C_n t^{\lambda_n - 3} + D_n t^{-\lambda_n - 1}) \frac{\phi_1^{(n)}}{\lambda_n(\lambda_n - 2)}.$$

dominated by the term $\frac{1}{16}t^3 f(\theta,\beta)$, except at the edges and the effect of the eddies on the interior flow is small.

In figures 2 and 3 we have plotted the level lines in the reference configuration of the stream function $\Psi(t,\theta)$ giving the edge eddies and the physical stream function $\psi(t,\theta)$ for $2\beta = 60°$. Figure 4 shows edge eddies for $2\beta = 10°$. When $2\beta \to 0$ the number of edge eddies increases without bound; this limit can be made to coincide with the problem studied by Joseph & Sturges (1975). We have already noted that the most persistent eddies, those for which $\mathrm{Re}\,\lambda_n$ is smallest, $\lambda_1, \lambda_2, \ldots$, in that order, disappear sequentially as 2β is increased beyond 146°. All of the eigenvalues λ_n are real when $2\beta > 180°$.

6. Convection in sectorial rings

We are now considering problem (3.14) when $a > 0$. The solution of this problem is given by (5.1). The constants C_n and D_n may be determined from the edge conditions. The edge condition at the top is (5.2) and this may be expressed as in (5.4) with C_n replaced by $C_n + D_n$:

$$\frac{1}{16}\begin{pmatrix} 3f(\theta,\beta) \\ -K \cos\theta - 3K_2 \cos\theta(3\sin^2\theta - 1) + 2\cos\theta - \theta\sin\theta \end{pmatrix}$$

$$= \sum_{-\infty}^{\infty} (C_n + D_n)\begin{pmatrix} \phi_1^{(n)} \\ \phi_2^{(n)} \end{pmatrix}. \quad (6.1)$$

θ	$\frac{10^3\times f(\theta,\beta)}{16}$	$N=1$	$N=3$	$N=5$	$N=9$	$N=10$
			On the top: $t=1$			
0°	4·11875	4·13268	4·11848	4·11868	4·11874	4·11876
6°	3·78008	3·79223	3·78074	3·78014	3·78007	3·78008
12°	2·85819	2·86318	2·85780	2·85816	2·85817	2·85819
18·	1·62492	1·61867	1·62476	1·62489	1·62490	1·62492
24°	0·49930	0·49028	0·50014	0·49941	0·49928	0·49929
30°	0	0	0	0	0	0
			On the bottom: $t=0{\cdot}5$			
0°	4·11875	3·92173	4·11600	4·11932	4·11858	4·11875
6°	3·78008	3·66876	3·78001	3·77960	3·77991	3·78008
12°	2·85819	2·92578	2·86264	2·85839	2·85803	2·85819
18°	1·62492	1·79603	1·62171	1·62522	1·62478	1·62492
24°	0·49930	0·60184	0·49616	0·49840	0·49920	0·49930
30°	0	0	0	0	0	0

TABLE 6. Convergence of the top edge series (6.1) and the bottom edge series (6.2) when $2\beta = 60°$ and $a/b = 0{\cdot}5$.

$$\frac{\Psi}{t^3}\times 10^3 = \frac{10^3\times f(\theta,\beta)}{16} = 10^3\times \sum_{-N}^{N}(C_n t^{\lambda_n-3}+D_n t^{-\lambda_n-1})\frac{\phi_1^{(n)}}{\lambda_n(\lambda_n-2)}.$$

At the bottom, $r_0 = a = bt_0$, $t_0 = a/b$, $t_0 \ll 1$, we find that

$$\begin{pmatrix}\dfrac{\partial\Psi}{\partial t}\\ \Psi\end{pmatrix} = \frac{t_0^2}{16}f(\theta,\beta)\begin{pmatrix}3\\ t_0\end{pmatrix} = \sum_{-\infty}^{\infty}\begin{pmatrix}\left(\dfrac{C_n t_0^{\lambda_n-3}}{\lambda_n-2}-\dfrac{D_n t_0^{-\lambda_n-1}}{\lambda_n}\right)\phi_1^{(n)}\\ (C_n t_0^{\lambda_n-3}+D_n t^{-\lambda_n-1})\,\phi_2^{(n)}\end{pmatrix}. \tag{6.2}$$

Applying the biorthogonality conditions (5.10) and (5.11) to (6.1) we find that the coefficients C_n+D_n are given by

$$C_n+D_n = I_n/F_n, \tag{6.3}$$

as in (5.12), where F_n is given by (5.11) and I_n by (5.13a). Turning now to (6.2) we note that

$$\int_{-\beta}^{\beta}[\psi_1^{(n)},\psi_2^{(n)}]\begin{pmatrix}0 & -1\\ 1 & 2\end{pmatrix}\begin{pmatrix}\frac{3}{16}t_0^2 f(\theta,\beta)-\left(\dfrac{C_n t_0^{\lambda_n-3}}{\lambda_n-2}-\dfrac{D_n t_0^{-\lambda_n-1}}{\lambda_n}\right)\phi_1^{(n)}\\ (t_0^3/16)f(\theta,\beta)-(C_0 t_0^{\lambda_n-3}+D_n t^{-\lambda_n-1})\,\phi_2^{(n)}\end{pmatrix}d\theta = 0. \tag{6.4}$$

Evaluation of (6.4), followed by elimination of $C_n = -D_n+I_n/F_n$ in the resulting expression, leads to the following expression for the coefficients D_n:

$$F_n D_n(t_0^{\lambda_n-3}-t_0^{-\lambda_n-1})+\sum_{l=-\infty}^{\infty}D_l B_{ln}\left(t_0^{\lambda_l-3}+\frac{(\lambda_l^2-\lambda_l-2)}{\lambda_l(3-\lambda_l)}t_0^{-\lambda_l-1}\right)$$
$$= I_n(t_0^{\lambda_n-3}-1)+\sum_{l=-\infty}^{\infty}\frac{I_l}{F_l}B_{ln}t_0^{\lambda_l-3}, \tag{6.5}$$

where
$$B_{ln} = \frac{3-\lambda_l}{\lambda_l-2}\int_{-\beta}^{\beta}\psi_2^{(n)}\phi_1^{(l)}d\theta, \quad n = \pm 1, \pm 2, \ldots.$$

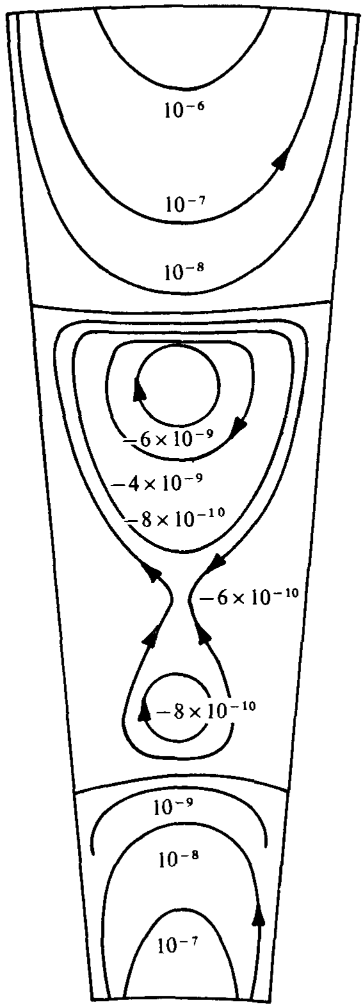

FIGURE 5. Edge eddies. $2\beta = 10°$, $a/b = 0{\cdot}5$.

Equations (6.5) form an infinite set of algebraic equations for the coefficients D_n. We solved (6.5) by truncation and checked the convergence of the truncated solution numerically. In all cases, the convergence was rapid (see tables 5 and 6 for representative examples).

In figures 5 and 6 we have plotted the level lines in the reference configuration of the stream function $\Psi(t, \theta)$ giving the edge eddies and the physical stream function $\psi(t, \theta)$ for the sectorial ring with $a/b = 0{\cdot}5$ when $2\beta = 10°$ and $2\beta = 60°$.

7. The shape of the free surface and the secondary motion in the deformed domain

The shape of the free surface is determined by the requirement (2.3d) that the jump in the normal component of the stress should be balanced by surface tension. At first

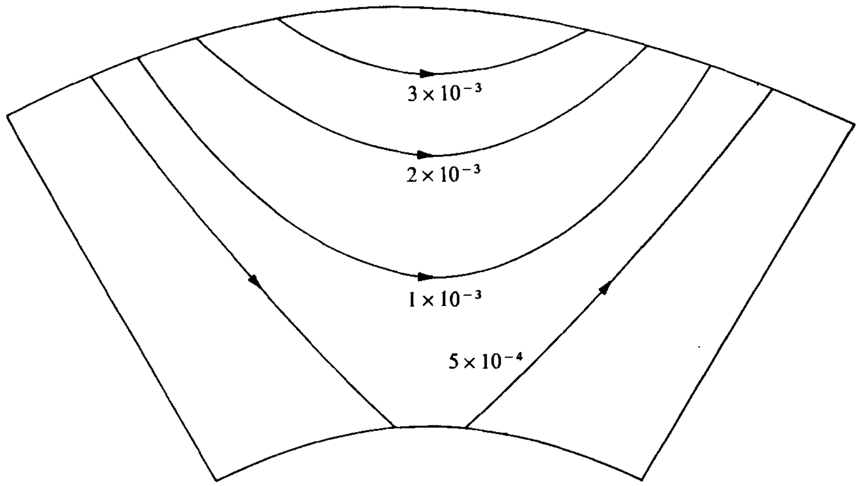

FIGURE 6. Edge eddies. $2\beta = 60°$, $a/b = 0{\cdot}5$.

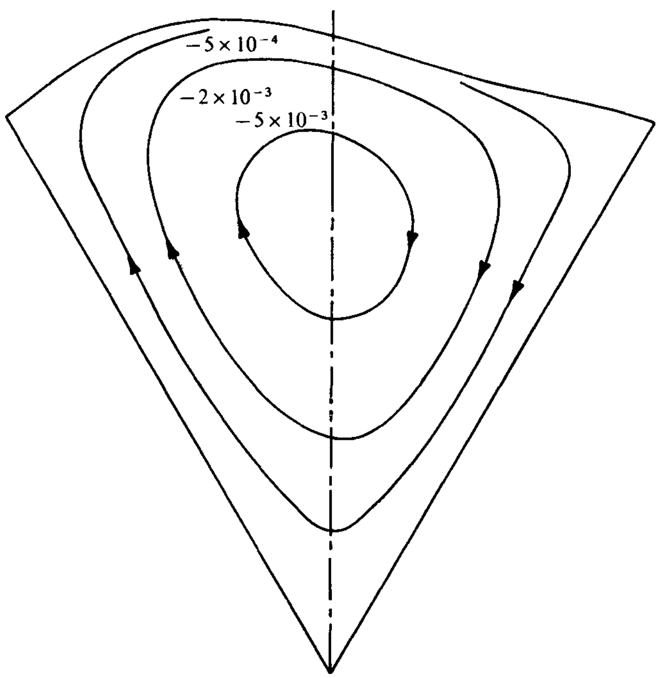

FIGURE 7. Streamlines in the deformed domain $\mathscr{V}_\epsilon$ when a fixed contact line boundary condition is assumed. The streamlines in the reference domain are shown in figure 3.

order this condition may be written as

$$\mu\frac{\partial u_r^{\langle 1\rangle}}{\partial r_0} - \Phi^{\langle 1\rangle} + \sigma(R^{\langle 1\rangle} + R^{\langle 1\rangle}_{,\theta\theta})/R_0^2 + \rho g R^{\langle 1\rangle}\cos\theta = 0 \tag{7.1}$$

on $r_0 = R_0$. This equation is to be solved relative to side-wall boundary conditions arising from (2.4a, b),

$$R^{\langle 1\rangle}(\pm\beta) = 0 \quad \text{or} \quad R^{\langle 1\rangle}_{,\theta}(\pm\beta) = 0, \tag{7.2}$$

θ	$H \times 10^3$	$H \times 10^3$
0°	0	0
3°	0·2494	0·6079
6°	0·4787	1·195
9°	0·6686	1·740
12°	0·8021	2·226
15°	0·8648	2·638
18°	0·8468	2·963
21°	0·7434	3·198
24°	0·5576	3·343
27°	0·3012	3·411
30°	0	3·425

TABLE 7. The correction coefficients H for the free surface on a liquid in a sectorial cavity with wedge angle 2β of 60°. The first column is for adhesive contact $H(\pm\beta) = 0$. The second column is for flat contact problem, $H'(\pm\beta) = 0$.

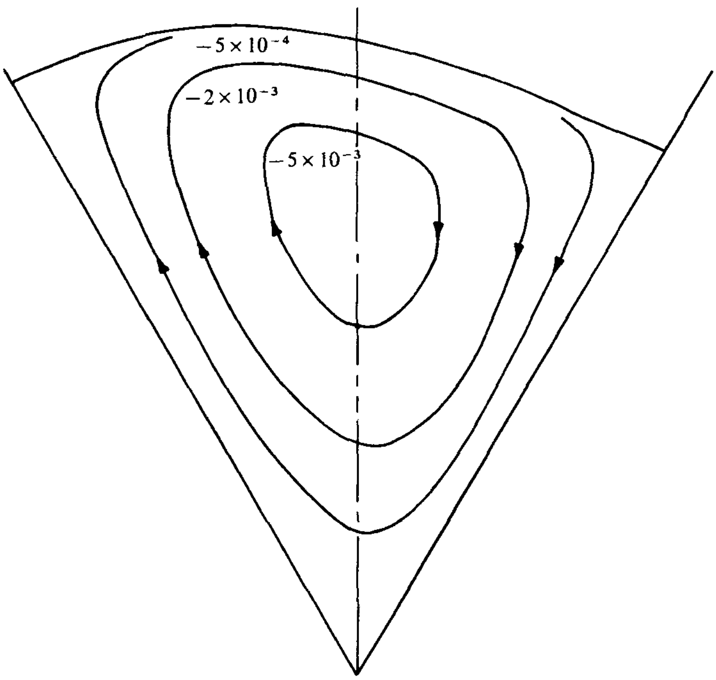

FIGURE 8. Streamlines in the deformed domain $\mathscr{V}_\epsilon$ when a fixed angle of perpendicular contact is assumed. The streamlines in the reference domain are shown in figure 3.

and a volume conservation condition

$$\int_{-\beta}^{\beta} R^{\langle 1\rangle}\, d\theta = 0. \tag{7.3}$$

To compute $R^{\langle 1\rangle}$ from (7.1) we must first find the function $\Phi^{\langle 1\rangle}$; the radial component of velocity $u_r^{\langle 1\rangle}$ may be obtained by differentiating the stream function. Since $\mathbf{u}^{\langle 1\rangle}$ is known, we may obtain $\Phi^{\langle 1\rangle}$ by integrating (3.9). After writing equations in terms of the dimensionless quantities introduced in (3.13a) with

$$\mathscr{P} = \frac{\beta}{\rho g \alpha R}\,\Phi^{\langle 1\rangle}$$

and

$$H = \frac{\sigma\beta}{\rho\alpha g R_0^3}\,R^{\langle 1\rangle},$$

we find that

$$\mathscr{P}(t,\theta) = -2\sum_{-\infty}^{\infty}\frac{C_n(\lambda_n-1)}{\lambda_n(\lambda_n-2)}\,t^{\lambda_n-2}\cos\lambda_n\beta\sin(\lambda_n-2)\,\theta-\tfrac{1}{4}t[(K_1+\tfrac{3}{4}K_2-\tfrac{3}{4})\cdot\sin\theta+\theta\cos\theta]+A_1,$$

where A_1 is a constant, and

$$H''+H+\tfrac{1}{16}[(2K_1-3K_2-1)\sin\theta+6\theta\cos\theta+6\sin^3\theta]$$
$$+\sum_{-\infty}^{\infty}C_n\left\{\frac{\lambda_n-1}{\lambda_n-2}\cos(\lambda_n-2)\,\beta\sin\lambda_n\theta+\frac{(\lambda_n-1)(4-\lambda_n)}{\lambda_n(\lambda_n-2)}\cos\lambda_n\beta\sin(\lambda_n-2)\,\theta\right\}=0. \quad (7.4)$$

The general solution of (7.4) is

$$\begin{aligned}H = {} & ((1-2K_1+3K_2)\sin\theta+3K_2\sin^3\theta-6\theta^2\sin\theta\\ & +(4K_1+3K_2-8)\,\theta\cos\theta)/64\\ & -2\,\mathrm{Re}\sum_{n=1}^{\infty}C_n((\lambda_n-4)\cos\lambda_n\beta\sin(\lambda_n-2)\,\theta/\lambda_n(\lambda_n-2)(\lambda_n-3)\\ & -\cos(\lambda_n-2)\,\beta\sin\lambda_n\theta/(\lambda_n+1)(\lambda_n-2))\\ & +B_1\cos\theta+B_2\sin\theta+A_1. \end{aligned} \quad (7.5)$$

The constants B_1, B_2 and A_1 may be determined from equations following from (7.2) and (7.3). When $H(\pm\beta)=0$, then $A_1=B_1=0$ and

$$\begin{aligned}B_2 = {} & \frac{1}{64}\left(2K_1-3K_2-1+6\beta^2-3K_2\sin^2\beta+(8-4K_1-3K_2)\frac{\beta\cos\beta}{\sin\beta}\right)\\ & +\frac{1}{\sin\beta}\,\mathrm{Re}\sum_{n=1}^{\infty}C_n\left(\frac{(\lambda_n-4)}{\lambda_n(\lambda_n-2)(\lambda_n-3)}\cos\lambda_n\beta\sin(\lambda_n-2)\,\beta\right.\\ & \left.-\frac{1}{(\lambda_n+1)(\lambda_n-2)}\cos(\lambda_n-2)\,\beta\sin\lambda_n\beta\right).\end{aligned}$$

When $H'(\pm\beta)=0$, then $A_1=B_1=0$ and

$$\begin{aligned}B_2 = {} & \frac{1}{64}\left(7-2K_1-6K_2+6\beta^2+9K_2\sin^2\beta+(4+4K_1+3K_2)\frac{\beta\sin\beta}{\cos\beta}\right)\\ & +\frac{1}{\cos\beta}\,\mathrm{Re}\sum_{n=1}^{\infty}C_n\left(\frac{4(4+\lambda_n-\lambda_n^2)}{\lambda_n(\lambda_n+1)(\lambda_n-2)(\lambda_n-3)}\cos\lambda_n\beta\cos(\lambda_n-2)\,\beta\right).\end{aligned}$$

Numerical values of the correction coefficient H are given in table 7.

The correction coefficient allows us to compute the shape of the free surface when ϵ is small. We may then, following procedures of the Lagrangian theory of domain perturbations (Joseph & Sturges 1975), obtain the level lines of the stream function in the deformed domain by inverting the scaling transformation (3.4). In figures 7 and 8 we show how different boundary conditions for H induce a different scaling (3.4) of the streamline patterns (figure 3) in the reference domain.

This work was supported by the U.S. Army Research Office and under NSF grant 19047. A portion of this work is taken from a Master's degree paper by C. H. Liu. The theoretical ideas and asymptotic analysis are due to D. Joseph while most of the calculations and all of the numerical computations are due to C. H. Liu.

REFERENCES

DEAN, W. R. & MONTAGNON, P. E. 1949 On the steady motion of viscous liquid in a corner. *Proc. Camb. Phil. Soc.* **45**, 389.

HARDY, G. H. 1902 On the zeros of the integral function
$$x-\sin x = \sum_{n=1}^{\infty} (-1)^{n-1}\frac{x^{n^2\pm 1}}{2n+1\,!}.$$ *Mess. Math.* **31**, 161.

JOSEPH, D. D. 1974 Slow motion and viscometric motion. Stability and bifurcation of the rest state of a simple fluid. *Arch. Rat. Mech. Anal.* **56**, 99.

JOSEPH, D. D. 1977 The convergence of biorthogonal series for biharmonic and Stokes flow edge problems. Part 1. *SIAM J. Appl. Math.* (to appear).

JOSEPH, D. D. & FOSDICK, R. L. 1973 The free surface on a liquid between cylinders rotating at different speeds. Part I. *Arch. Rat. Mech. Anal.* **49**, 321.

JOSEPH, D. D. & STURGES, L. 1975 The free surface on a liquid filling a trench heated from its side. *J. Fluid Mech.* **69**, 565.

JOSEPH, D. D. & STURGES, L. 1977 The convergence of biorthogonal series for biharmonic and Stokes flow edge problems. Part 2. *SIAM J. Appl. Math.* (to appear).

LIU, C. H. & JOSEPH, D. D. 1977 Stokes flow in conical cavities. *SIAM J. Appl. Math.* (to appear).

MOFFATT, H. K. 1964 Viscous and resistive eddies near a sharp corner. *J. Fluid Mech.* **18**, 1.

SATTINGER, D. H. 1976 On the free surface of a viscous fluid motion. *Proc. Roy. Soc.* A **349**, 183.

SMITH, R. C. T. 1952 The bending of a semi-infinite strip. *Aust. J. Sci. Res.* **5**, 227.

STURGES, L. & JOSEPH, D. D. 1977 The free surface on a simple fluid between cylinders undergoing torsional oscillations. Part III. Oscillating planes. *Arch. Rat. Mech. Anal.* (to appear).

YOO, J. Y. & JOSEPH, D. D. 1977 Stokes flow in a trench between concentric cylinders. *SIAM J. Appl. Math.* (to appear).